

Non-Markovian coherence dynamics of driven spin boson model: damped quantum beat or large amplitude coherence oscillation

Xiufeng Cao*, Hang Zheng

*Department of Physics, Shanghai Jiaotong University,
Shanghai 200240, People's Republic of China*

Abstract

The dynamics of driven spin boson model is studied analytically by means of the perturbation approach based on a unitary transformation. We gave the analytical expression for the population difference and coherence of the two level system. The results show that in the weak driven case, the population difference present damped coherent oscillation (single or double frequency) and the frequencies depend on the initial state. The coherence exhibit damped oscillation with Rabi frequency. When driven field is strong enough, the population difference exhibit undamped large-amplitude coherent oscillation. The results easily return to the two extreme cases without dissipation or without periodic driven.

Key word: dissipation, driving, decoherence

PACS numbers: 03.65.Yz, 03.67.Lx, 03.67.Pp

* Email: cxf@sjtu.edu.cn

1. Introduction

Discrete electronic states of the qubits can be considered as localized two levels systems (TLS), which has been related to the potential use as building blocks of prospective quantum logic gates [1, 2]. Solid-state qubits, including superconducting [3, 4, 5, 6] and semiconductor[7, 8, 9, 10] ones, couple to environmental degrees of freedom that potentially lead to dephasing. The development of techniques to protect coherence of carrier tunneling in the qubits are key points for a successful implementation of quantum information processing in these systems and the development of qubit based quantum information systems.

Since the development of local spectroscopy techniques, the atomiclike optical properties of semiconductor quantum dots (charge qubit) or superconductive ring (flux qubit) have been intensively studied. The group of T. H. Stievater have reported the first observation of Rabi oscillations from excitons confined to single GaAs/Al_{0.3}Ga_{0.7}As QD[11]. L. Besombes *et al.* optically control the charge state of a single QD and coherently manipulate the confined wave function exploiting quantum interference and Rabi oscillation phenomena by microspectroscopy in individual InGaAs/GaAs QDs[12]. Using a pulse technique, Pashkin *et al.* coherently mix quantum states and observe quantum coherent oscillation of coupled qubits in the vicinity of the co-resonance[13], the spectrum of which reflects interaction between the qubits. Zrenner *et al.* actualize Rabi oscillation by playing an InGaAs quantum dot in a photodiode and demonstrate that coherent optical excitations in the quantum dot two level system can be converted into deterministic photocurrents[14]. While many-body effects of the environment fundamentally change many aspects of Rabi oscillations, particularly the lack of saturation or decoherence. Thus, we think over two questions: first, how does the interplay or competition between optical driving and dissipation in the TLS influence the decoherence? second, can one sustain large-amplitude coherent oscillation in driven spin boson model? A good knowledge of the decoherence holds most prominently for many applications such as optoelectronic devices in quantum information processing where the operation completely relies on the presence of coherence[15].

The dynamics of driven spin-boson model[16] also attract theoretical physics attention for its widespread applications to various biological, chemical, and physical systems, e.g., ac-driven superconducting quantum interference devices, laser-induced isomerization of bistable molecules, laser-induced localization of electrons in semiconductor double-well quantum structures, or paraelectric resonance. The various communities typically rely on different

methods of description. The most direct approach is portrayal of the time evolution of the corresponding reduced density matrix $\rho(t)$, which starts from the generalized master equation (GME) of the TLS. Two popular approximations are either based on the system-bath coupling expansion obtained by use of a projector operator method (commonly known as the Bloch-Redfield formalism[17]), or on the expansion in the coupling expansion in the coupling matrix element Δ (such as a tunnel splitting) by use of (real-time) path-integral methods, such as the application of the so termed noninteracting blip approximation (NIBA[18]). Ludwig Hartmann *et al.* have enlightened the advantages and disadvantages of two approaches[19]. A special case where the field frequency is comparable to the TLS frequency (resonance or near-resonance) is prominent important in experiment, but is more difficult to handle analytically. If the system-bath coupling is weak, the traditional optical Bloch equations will produce a meaningful result[20, 21]. However, their model with decoherence rate as a constant parameter is too simple to make detailed quantitative predictions here[22]. In general, to obtain a solution for time-dependent spin-boson problems even numerically is nontrivial task[23, 24].

In this paper we study the quantum dynamics of driven spin-boson model, where the driven field is near resonance with the TLS. Analytical explicit expressions for population difference $\langle\sigma_z(t)\rangle$ and coherence $\langle\sigma_x(t)\rangle$ are presented through perturbation treatment based on a unitary transformation. The result shows that with increasing amplitude of the driven field, the population difference transferred from damped quantum oscillation (single-frequency or double-frequency) to large amplitude undamped coherent oscillation. Therefore, one can efficiently control quantum coherent dynamic by optical pulse, induce and maintain large-amplitude coherent oscillations. The critical condition from damped to undamped large-amplitude coherent oscillations is given. The coherence decays to ground state with the Rabi frequency in the case of weak driven. We also investigated the dependence of the population difference $\langle\sigma_z(t)\rangle$ and coherence $\langle\sigma_x(t)\rangle$ on the initial state.

The paper is organized as follows: In sec 2 we introduce the model Hamiltonian for driven spin-boson model and solve it in terms of a perturbation treatment based on unitary transform. We analyze the population difference and the coherence in different initialization and give discussion in sec 3. Finally, the conclusion is given in sec 4.

2. The model and theory

We study the driven spin-boson dynamics, where the two level system is linearly coupled

to a continuum of harmonic oscillators and is driven by classical microwave field. The system under consideration can be modeled by the Hamiltonian[18, 21]:

$$H(t) = H_s + H_d(t) + H_b + H_i \quad (1)$$

with

$$H_s = -\Delta\sigma_x/2 \quad (2)$$

$$H_d(t) = \varepsilon(t)\sigma_z \quad (3)$$

$$H_b = \sum_k \omega_k b_k^\dagger b_k \quad (4)$$

$$H_i = \frac{1}{2} \sum_k g_k (b_k^\dagger + b_k) \sigma_z \quad (5)$$

where H_s is the Hamiltonian of the TLS, $H_d(t)$ of the external driven field, H_b of the bath and H_i of bath and system interaction that is responsible for decoherence. Throughout this paper we set $\hbar = 1$. Here σ_i are pauli spin matrices, Δ describe the coupling between the two state and $\varepsilon(t)$ is the external time dependent modulated field. b_k^\dagger (b_k) and ω_k are the creation (annihilation) operator and energy of the phonons with the wave vector k . g_k is the electron-phonon coupling strength. The ohmic bath is characterized by its spectral density:

$$J(\omega) = \sum_k g_k^2 \delta(\omega - \omega_k) = 2\alpha\omega\theta(\omega_c - \omega) \quad (6)$$

where α is the dimensionless coupling constant and $\theta(x)$ is the usual step function.

Firstly we diagonalize the Hamiltonian independent of time $H_s + H_b + H_i$. Here we apply a canonical transformation, $H' = \exp(s)H \exp(-s)$ with the generator[25]:

$$S = \sum_k \frac{g_k}{2\omega_k} \xi_k (b_k^\dagger - b_k) \sigma_z \quad (7)$$

Thus we get the Hamiltonian H' and decompose it into three parts:

$$H' = H'_0 + H'_1 + H'_2 \quad (8)$$

where

$$H'_0 = -\frac{1}{2}\eta\Delta\sigma_x + \sum_k \omega_k b_k^\dagger b_k - \sum_k \frac{g_k^2}{4\omega_k} \xi_k (2 - \xi_k^+) \quad (9)$$

$$H'_1 = -\frac{1}{2} \sum_k g_k (1 - \xi_k^+) (b_k^+ + b_k) \sigma_x - i \frac{\eta \Delta}{2} \sigma_y \sum_k \frac{g_k}{\omega_k} \xi_k^+ (b_k^+ - b_k) \quad (10)$$

$$\begin{aligned} H'_2 = & -\frac{1}{2} \Delta \sigma_x (\cosh(\sum_k \frac{g_k}{\omega_k} \xi_k^+ (b_k^+ - b_k)) - \eta) \\ & - i \frac{\Delta}{2} \sigma_y (\sinh(\sum_k \frac{g_k}{\omega_k} \xi_k (b_k^+ - b_k)) - \eta \sum_k \frac{g_k}{\omega_k} \xi_k^+ (b_k^+ - b_k)) \end{aligned} \quad (11)$$

with

$$\eta = \exp(-\sum_k \frac{g_k^2}{2\omega_k^2} \xi_k^2) \quad (12)$$

$$\xi_k = \frac{\omega_k}{\omega_k + \eta \Delta} \quad (13)$$

Obviously, H'_0 can be solved exactly. We denote the ground state of H'_0 as $|g\rangle = |s_1\rangle |\{0_k\}\rangle$, and the lowest excited states as $|s_2\rangle |\{0_k\}\rangle$, $|s_1\rangle |\{1_k\}\rangle$ where $|s_1\rangle$ and $|s_2\rangle$ are eigenstates of σ_x ($\sigma_x |s_1\rangle = |s_1\rangle$, $\sigma_x |s_2\rangle = -|s_2\rangle$), $|\{n_k\}\rangle$ means that there are n_k phonons for mode k . The last term of H'_0 is constant energy and has no effect to the dynamics behavior. Thus, we can diagonalize the lowest excited states H' as:

$$H' = -\frac{1}{2} \eta \Delta |g\rangle \langle g| + \sum_E E |E\rangle \langle E| + \text{terms with higher excited states} \quad (14)$$

The digitalization is through the following transformations[25]

$$|s_2\rangle |\{0_k\}\rangle = \sum_E x(E) |E\rangle \quad (15)$$

$$|s_1\rangle |\{1_k\}\rangle = \sum_E y_k(E) |E\rangle \quad (16)$$

$$|E\rangle = x(E) |s_2\rangle |\{0_k\}\rangle + \sum_k y_k(E) |s_1\rangle |\{1_k\}\rangle \quad (17)$$

where

$$x(E) = (1 + \sum_k \frac{V_k^2}{(E + \frac{1}{2} \eta \Delta - \omega_k)^2})^{\frac{1}{2}} \quad (18)$$

and

$$y_k(E) = \frac{V_k}{E + \frac{1}{2} \eta \Delta - \omega_k} x(E) \quad (19)$$

with $V_k = \eta \Delta g_k \xi_k / \omega_k$. E are the diagonalized excitation energy and they are solutions of the equation

$$E - \frac{1}{2}\eta\Delta - \sum_k \frac{V_k^2}{E + \frac{1}{2}\eta\Delta - \omega_k} = 0 \quad (20)$$

A series of experiments have successfully realized coherent control of the qubit by applying resonant microwave excitations[3]. The qubit state evolves driven by a time-dependent term $\varepsilon_{mw} \cos(2\pi Ft) \sigma_z$ in the Hamiltonian, where F is the microwave frequency and ε_{mw} is the microwave amplitude. So we focus our attention on a monochromatic field of the form $\varepsilon(t) = \varepsilon \cos(\Omega t) \sigma_z$ and choose the control field excitation to be resonant with the splitting of the tunneling TLS such that it also does not induce transition to higher-lying excitation. So Hamiltonian can approximately be describes as:

$$H' = -\frac{1}{2}\eta\Delta|g\rangle\langle g| + \sum_E E|E\rangle\langle E| - \varepsilon \cos(\Omega t) \sigma_z \quad (21)$$

After expand with eigenstate $|g\rangle$ and $|E\rangle$:

$$H' = -\frac{1}{2}\eta\Delta|g\rangle\langle g| + \sum_E E|E\rangle\langle E| - \frac{\varepsilon}{2} \sum_E (x^*(E)|g\rangle\langle E| \exp(i\Omega t) + x(E)|E\rangle\langle g| \exp(-i\Omega t)) \quad (22)$$

In deriving Eq.22 we have ignored the nonenergy conserving term or counter rotation term in the rotation wave approximation[26]. This is generally a very good approximation, especially in the special case when the two states are at resonance or near resonance with the incident field $\Delta \approx \Omega$. In the interaction picture,

$$H'_{0I} = -\frac{1}{2}\eta\Delta|g\rangle\langle g| + \sum_E E|E\rangle\langle E| \quad (23)$$

$$\begin{aligned} V_I(t) = & -\frac{\varepsilon}{2} \sum_E (x^*(E)|g\rangle\langle E| \exp(i(-\frac{1}{2}\eta\Delta - E + \Omega)t) \\ & + x(E)|E\rangle\langle g| \exp(-i(-\frac{1}{2}\eta\Delta - E + \Omega)t)) \end{aligned} \quad (24)$$

The wave function can be written in the form $|\Psi(t)\rangle = C_1(t)|g\rangle + \sum_E C_E(t)|E\rangle$, where $C_1(t)$ and $C_E(t)$ are the probability of find the particle in state $|g\rangle$ and $|E\rangle$ at time t , respectively. The corresponding Heisenberg equation is

$$\frac{d}{dt}|\Psi(t)\rangle = -iV_I(t)|\Psi(t)\rangle \quad (25)$$

Assumed that the initial state of the model is $\exp(S)|\Psi(0)\rangle = C_1(0)|s_1\rangle|\{0_k\}\rangle + C_2(0)|s_2\rangle|\{0_k\}\rangle = C_1(0)|g\rangle + C_2(0)\sum_E x(E)|E\rangle$. Using Laplace transformation, we obtain

$$C_0(P) = \frac{C_1(0) + C_2(0)\frac{\varepsilon}{2}\sum_E \frac{|x(E)|^2}{E-iP}}{P + i(-\frac{1}{2}\eta\Delta + \Omega) - i\frac{\varepsilon^2}{4}\sum_E \frac{|x(E)|^2}{E-iP}} \quad (26)$$

and

$$\sum_E x^*(E)C_E(P) = \frac{(C_2(0) * (P + i(-\frac{1}{2}\eta\Delta + \Omega)) + iC_1(0)\frac{\varepsilon}{2}) * -i\sum_E \frac{|x(E)|^2}{E-iP}}{P + i(-\frac{1}{2}\eta\Delta + \Omega) - i\frac{\varepsilon^2}{4}\sum_E \frac{|x(E)|^2}{E-iP}}. \quad (27)$$

In the complex function theory, the sum of E can be simplified:

$$\sum_E \frac{|x(E)|^2}{E-iP} = \frac{1}{2\pi i} \int \frac{dE}{(E - \frac{1}{2}\eta\Delta - \sum_k \frac{V_k^2}{E + \frac{1}{2}\eta\Delta - \omega_k})(E-iP)} \quad (28)$$

$$= -\frac{1}{iP - \frac{1}{2}\eta\Delta - \sum_k \frac{V_k^2}{iP + \frac{1}{2}\eta\Delta - \omega_k}} \quad (29)$$

After Changing $iP + \frac{1}{2}\eta\Delta$ to $\omega + i0^+$ [27], $C_0(P)$ and $\sum_E x^*(E)C_E(P)$ can be rewritten to:

$$C_0(\omega) = \frac{i(\omega - \eta\Delta - R(\omega) + i\gamma(\omega))C_1(0) - iC_2(0)\frac{\varepsilon}{2}}{(\omega - \Omega)(\omega - \eta\Delta - R(\omega) + i\gamma(\omega)) - \frac{\varepsilon^2}{4}} \quad (30)$$

and

$$\sum_E x^*(\omega)C_E(\omega) = \frac{i(\omega - \Omega)C_2(0) - iC_1(0)\frac{\varepsilon}{2}}{(\omega - \Omega)(\omega - \eta\Delta - R(\omega) + i\gamma(\omega)) - \frac{\varepsilon^2}{4}} \quad (31)$$

where $R(\omega)$ and $\gamma(\omega)$ denote the real and imaginary parts of $\sum_k V_k^2/(\omega - \omega_k)$,

$$R(\omega) = -2\alpha \frac{(\eta\Delta)^2}{\omega + \eta\Delta} \left\{ \frac{\omega_c}{\omega_c + \eta\Delta} - \frac{\omega}{\omega + \eta\Delta} \ln \left[\frac{|\omega|(\omega_c + \eta\Delta)}{\eta\Delta(\omega_c - \omega)} \right] \right\} \quad (32)$$

and

$$\gamma(\omega) = 2\alpha\pi\omega \frac{(\eta\Delta)^2}{(\omega + \eta\Delta)^2} (\theta(\omega) + \theta(\omega_c - \omega) - 1) \quad (33)$$

Comparing with Bloch equation and Markovian approximation, decoherence rates $\gamma(\omega)$ become frequency dependent themselves. $R(\omega)$ is determined by the whole of the spectrum of frequencies in the spectral density $J(\omega)$ of the ohmic bath. According to the correlation of real and imaginary parts in complex function theory, $\gamma(\omega)$ also involve the whole of the spectrum of frequencies in the spectral density $J(\omega)$ of the ohmic bath. That is more general and physical.

Then we inverse Laplace transformation to time parameter space:

$$C_0(t) = \frac{\exp(i\eta\Delta t/2)}{2\pi} \int_{-\infty}^{+\infty} C_0(\omega) \exp(-i\omega t + 0^+) d\omega \quad (34)$$

and

$$\sum_E x^*(\omega) C_E(t) = \frac{\exp(i\eta\Delta t/2)}{2\pi} \int_{-\infty}^{+\infty} \sum_E x^*(\omega) C_E(\omega) \exp(-i\omega t + 0^+) d\omega. \quad (35)$$

The expectation value σ_i can be expressed as:

$$\langle \sigma_i(t) \rangle = \langle \Psi(0) | \sigma_i(t) | \Psi(0) \rangle = \langle \Psi(0) | \exp(-S) \exp(-iH't) \sigma_i \exp(iH't) \exp(S) | \Psi(0) \rangle \quad (36)$$

After straightforward calculation, the electron population difference $\langle \sigma_z(t) \rangle$ and the coherence $\langle \sigma_x(t) \rangle$ are gained as follows:

$$\langle \sigma_z(t) \rangle = 2\text{Re}(C_0^*(t) \sum_E x^*(\omega) C_E(t) \exp(-i\Omega t)) \quad (37)$$

and

$$\langle \sigma_x(t) \rangle = \eta * (1 - 2 \sum_E x^*(\omega) C_E(t) \sum_{E'} x^*(\omega) C_{E'}(t)). \quad (38)$$

Rather simple expression for the population and coherence are obtained analytically.

3. The result and discussion

Here we only discuss the near resonant case $\Omega = \Delta$. ω_c is taken as the energy unit. Without special indication, the coupling constant of the environment and TLS is taken as $\alpha = 0.01$.

In the especial case without coupling to the environment, we rotate σ_z axis around σ_y axis to σ_x axis, correspondingly σ_x axis to σ_z axis, the Hamiltonian turn into the famous quantum optics model describing the interaction of a single-mode radiation with a two-level atom[26]. As we have known, the dynamics of $\langle \sigma_z(t) \rangle$ depend on the initial condition. If the qubit is at $\langle \sigma_x(t=0) \rangle = 1$ eigenvalue, the driven field is turned on, then, using the rotating wave approximation, i.e. in the near resonance condition, the population difference $\langle \sigma_z(t) \rangle$ will exhibit quantum beats that result from the interference of fast oscillation with field frequency Ω and slow oscillations with Rabi frequency ε . The coherence $\langle \sigma_x(t) \rangle$ oscillates with the Rabi frequency. But if the system is initially in the state $\langle \sigma_z(t=0) \rangle = 1$, without the environment, $\langle \sigma_z(t) \rangle$ will present $\cos \Omega t$ oscillation and $\langle \sigma_x(t) \rangle = 0$. We also knew that in the other especial case lack of the driven field, $\langle \sigma_z(t) \rangle$ damply oscillate [25]. The question

is how will this dissipation environment and driven field collectively influence the population difference and coherence of TLS.

In Fig. 1, we plot coherent dynamics of the population difference $\langle\sigma_z(t)\rangle$ in the initial state $\langle\sigma_z(t=0)\rangle = 1$, where a driving field is of the same frequency $\Omega = \Delta$, but of different amplitude. The curves shown in panels (a), (b) and (c) correspond to three external field amplitude $\varepsilon = 0, 0.01, 0.1$. Fig. 1(d) present population difference $\langle\sigma_z(t)\rangle$ with $\varepsilon = 0.4$ and $\alpha = 0.3$. The Fourier spectrums of the population difference are presented in the right four corresponding left panels of Fig. 1. As seen from Fig. 1(a), in the absence of driven, population difference exhibits damped oscillation. The frequency ω_0 and damping rate γ of the oscillations is well agree with previous result[25]. With weak driving field strength, $\langle\sigma_z(t)\rangle$ decays with beat pattern in Fig. 1(b) of two frequency almost $\Omega - \varepsilon$ and Ω . Further increasing driving field strength over the regime of half-width γ of the driving frequency Ω , $\langle\sigma_z(t)\rangle$ damped oscillate with a master frequency Ω in Fig. 1(c). Above three case shows that in the weak driven case, the system is always damped and this genuine quantum coherence oscillation is weakened by friction from the dissipation environment. For sufficiently strong amplitude $\varepsilon \geq 2\Omega$, population difference damped a little at initial short time, then present undamped large-amplitude coherent oscillations with the frequency of the incident field Ω . That is to say, the driven field overcome dissipation and domain the dynamics of the system. It is clearly seen that quantum beat pattern of the population difference $\langle\sigma_z(t)\rangle$ oscillate only appears in the small regime of driving strength, which is depend on the frequency $\Omega - \varepsilon$ and/or $\Omega + \varepsilon$ whether moves out of the spectral width γ of the incident field Ω or not.

In Fig. 2, the expectation value $\langle\sigma_x(t)\rangle$ plotted as a function of $\omega_c t$ for TLS driven by a monochromatic field with the same parameters as in Fig. 1. As seen, in the absence of driving, the coherence $\langle\sigma_x(t)\rangle$ reaches asymptotically a value 1, implying that mainly the ground state is occupied at long times[28]. For weak driving amplitude $\varepsilon = 0.01$ and 0.1 , it is visible that $\langle\sigma_x(t)\rangle$ oscillated tends to 1 and the oscillation frequency is the Rabi frequency, which is directly proportional to driven amplitude. While for large driven field strength $\varepsilon = 0.4$, the coherence $\langle\sigma_x(t)\rangle$ oscillates around zero with a small amplitude. Driven field make the transfer probability to left state and right state equal, that is to say the electron tunnel between the two states left dot state $|L\rangle$ and right state $|R\rangle$, so the undamped oscillation occurs as seen in Fig. 1(d). The situation of strong driving field can be correspond to the case of absence of damping, where the coherence $\langle\sigma_x(t)\rangle$ is exactly equal to zero.

Since any superposition $|\Psi\rangle = \alpha|s1\rangle + \beta|s2\rangle$ can be prepared in experiment, through manipulation of the quantum state is performed by applying microwave pulses $\mu(t)$ to the gate[29]. Fig. 3 gives the population difference $\langle\sigma_z(t)\rangle$ for the same parameters as in Fig. 1, but assume that at time $t = 0$ the particle is held at superposition $\langle\sigma_x(t = 0)\rangle = 1$, with the bath being in thermal equilibrium. Without driven field, $\langle\sigma_z(t)\rangle = 0$. For weak driven, despite the dissipation we were able to induce Rabi oscillations by applying microwave pulses at the near-resonance frequency of the TLS. The oscillation decay nonexponentially and display a clear beating. From the Fourier spectrum, we find two oscillation frequency, one is the frequency of the incident field $\Omega - \varepsilon$ and the other is the Rabi frequency $\Omega + \varepsilon$, that is to say, $\langle\sigma_z(t)\rangle$ can be fitted by $\sin\varepsilon t * \sin\Omega t$. This corresponds to the common quantum beat in the quantum optics. The frequencies of population difference oscillation are dependent on the initial state. In Fig.3(d), a well-behaved coherent oscillations can be observed after adequate long time when the driven field strength is adequately strong $\varepsilon = 0.4$. The frequency of the oscillations firstly is $\Omega + \varepsilon$, then Ω .

In the same parameters and the initialization with Fig. 3, coherence $\langle\sigma_x(t)\rangle$ are plotted in Fig. 4. In the presence of tunneling with a dissipation bath and weak driven, due to the dominance of transitions to the continuum modes, we see that the coherence $\langle\sigma_x(t)\rangle$ presents damped oscillation and finally stabilizes the ground state as seem from the Fig. 4(a) and 4(b). The frequency of the oscillations is Rabi frequency. The damped can be look as a leakage of energy[30]. The leakage can be suppressed by enhancing of the external field. For strong driving field, the long time limit is shift to nonzero by external field.

The population difference $\langle\sigma_z(t)\rangle$ will exhibit damping quantum beat, which have be observed in superconducting qubit experiment[3]. Comparing Fig. 1 and Fig. 3, these curves show clearly that the initialization of TLS determine the features of the quantum beat. The condition to present beat in the initial state of Fig. 1 is more rigour than that of Fig. 3. The quantum beat only emerge in a small regime of the driving field amplitude, that is to say the driving field amplitude must be in the range of the damping rate γ of the driven frequency Ω . While in the initialization of Fig. 3, the quantum beat can always exist, except the driven amplitude enough strong to undamped oscillation. The frequency of the beat pattern Ω and $\Omega - \varepsilon$ or/and $\Omega + \varepsilon$ in Fig. 1, While in Fig. 3, the frequency of the beat pattern $\Omega - \varepsilon$ and $\Omega + \varepsilon$. It is helpful to experimenter for the empirical function choose. The difference of frequency in Fig.1 and Fig.3 is understood qualitatively as follows. In the initialization

$\langle \sigma_z(t=0) \rangle = 1$, $H_f(t) = \varepsilon(t)\sigma_z$ is the maximum of $H_f(t)$ but $H_i = \frac{1}{2} \sum_k g_k(b_k^+ + b_k)\sigma_z$ is zero due to $|\{n_k\}\rangle = |\{0_k\}\rangle$, so the driven field firstly domain the oscillation of TLS, then environment and driven field interplay. At the end the frequency of the oscillation give priority to Ω , only when $\Omega - \varepsilon$ or/and $\Omega + \varepsilon$ in the range of decoherence rate γ of the driving frequency Ω , quantum beat emerges. While in the initialization $\langle \sigma_x(t=0) \rangle = 1$, at the very start, $H_f(t) = \varepsilon(t)\sigma_z$ and $H_i = \frac{1}{2} \sum_k g_k(b_k^+ + b_k)\sigma_z$ are zero together, driving and bath interact so the frequency of the oscillation are $\Omega - \varepsilon$ and $\Omega + \varepsilon$.

In what follows, we give the transform condition from damped to undamped oscillation. From derivation, we can see that much of the behavior of the population difference $\langle \sigma_z(t) \rangle$ and coherence $\langle \sigma_x(t) \rangle$ can be learned from a study of the singularities of $C_0(\omega)$ and $\sum_E x^*(\omega)C_E(\omega)$. According the complex-function theory, we analyze the real part of the energy denominators, $\text{Re}D(\omega) = (\omega - \Omega)(\omega - \eta\Delta - R(\omega)) - \frac{\varepsilon^2}{4}$, that is symmetry in ε . Fig. 5 shows $\text{Re}D(\omega)$ with different driving field amplitude $\varepsilon = 0$ (solid line), 0.1 (dashed), 0.3 (dotted), 0.5 (dash-dotted). When $\varepsilon = 0$, the singularities of $C_0(\omega)$ and $\sum_E x^*(\omega)C_E(\omega)$ are $\omega = 0$ and $\omega = \omega_0$, which are correspond to zero drive and Lamb Shift due to the dissipation. ω_0 is determined by the function $\omega - \eta\Delta - R(\omega) = 0$ [25]. Owing to the driving field, two singularities are shift. Define the two singularities ω_1 and ω_2 and assume $\omega_1 < \omega_2$. We find that two positive singularities are in two sides of ω_0 in the case of small external driving field amplitude ε . With the increasing of ε , one pole ω_1 becomes larger and the other ω_2 becomes smaller, at the end the small singularity come to the negative axis. Furthermore, the imaginary parts of the denominator $\gamma(\omega)(\omega - \Omega)$ can be understood as a damping rate. Commonly, they depend on the frequency. Because of the interactions with the continuous spectral dissipation bath and driving field, the energy of the localized state is altered to new value ω_1 and ω_2 . The nature of the solution depends critically on whether the energy ω_1 and ω_2 are within the band of state ω_k . Therefore, the continuous band of state ω_k is confined to the range $0 < \omega_k < \omega_c$, so the character of solution determined whether ω_1 and ω_2 are also within this range. If the values are within the range $0 < \omega_1, \omega_2 < \omega_c$, the solution has an important property: dissipation domain the behavior in the system, after adequate time, the coherence oscillation is damped out. The reason is that generally imaginary component of denominator is not zero throughout the continuum band of photon, the decay rate $\gamma_1(\omega)$ and $\gamma_2(\omega)$ corresponding to ω_1 and ω_2 are finite. That is to say, the damping rate $\gamma(\omega)$ is nonzero if only in the section of $0 < \omega < \omega_c$, which is the key point of the result. Of course,

if one of the two energy ω_1 or ω_2 is outside of the band of continuum state, i.e. ω_1 is negative or $\omega_2 > \omega_c$, then the corresponding damping rate of the correspond energy vanishes. $\langle \sigma_z(t) \rangle$ can't decay to zero and always exhibits large amplitude coherent oscillation. The condition damped oscillation or not depend on two roots of $\text{ReD}(\omega)$ in the dissipation regime or not. Approximatively estimate when $\varepsilon \geq 2\Omega$, population difference can maintain undamped long coherence oscillation. We illuminate the possibility to induce and maintain large amplitude coherent oscillation by applying a resonant control field and present the condition of the long time coherence. It is favorable for quantum computation. The result is similar with Ref. 20.

4. Conclusion

In this paper, we have investigate the quantum optical control dynamics of the driven spin boson model by a perturbation treatment based on a unitary transformation. The population difference and coherence are obtained explicitly. Our approach is not restricted by the form of spectral density and the initialization. Additionally, a simple expression for the real part of the energy denominators, $(\omega - \Omega)(\omega - \eta\Delta - R(\omega)) - \frac{\varepsilon^2}{4}$, allows us to analyze the transform condition from damped quantum oscillation to undamped oscillation. We find that, for weak field, the population difference $\langle \sigma_z(t) \rangle$ presents damping quantum beat, while for strong field $\varepsilon \geq 2\Omega$, $\langle \sigma_z(t) \rangle$ preserve large amplitude coherent oscillation with the frequency Ω . The coherence $\langle \sigma_x(t) \rangle$ is also studied. Finally, we hope that this work will stimulate more experimental and theoretical works in quantum information and computation for quantum optical control.

Acknowledgments: This work was supported by the China National Natural Science Foundation (Grants No. 10474062 and No. 90503007).

-
- [1] Filippo Troiani, Ulrich Hohenester, and Elisa Molinari, Phys. Rev. B 62, R2263 (2000).
 - [2] Eliana Biolatti, Irene D'Amico, Paolo Zanardi, and Fausto Rossi, Phys. Rev. B. 65, 075306 (2002).
 - [3] P. Bertet, I. Chiorescu, G. Burkard, K. Semba, C. J. P. M. Harmans, D. P. DiVincenzo, and J. E. Mooij, Phys. Rev. Lett. **95**, 257002 (2005).

- [4] I. Chiorescu, Y. Nakamura, C. J. P. M. Harmans, and J. E. Mooij, *Science* **299**, 1869 (2003).
- [5] J. Claudon, F. Balestro, F. W. J. Hekking, and O. Buisson, *Phys. Rev. Lett.* **93**, 187003 (2004) .
- [6] T. Duty, D. Gunnarsson, K. Bladh, and P. Delsing, *Phys. Rev. B* **69**, 140503 (2004).
- [7] S. Gardelis, C. G. Smith, J. Cooper, D. A. Ritchie, E. H. Linfield, Y. Jin, and M. Pepper, *Phys. Rev. B* **67**, 073302 (2003).
- [8] L. C. L. Hollenberg, A. S. Dzurak, C. Wellard, A. R. Hamilton, D. J. Reilly, G. J. Milburn, and R. G. Clark, *Phys. Rev. B* **69**, 113301 (2004).
- [9] T. Hayashi, T. Fujisawa, H. D. Cheong, Y. H. Jeong, and Y. Hirayama, *Phys. Rev. Lett.* **91**, 226804 (2003) .
- [10] J. Gorman, D. G. Hasko, and D. A. Williams, *Phys. Rev. Lett.* **95**, 090502 (2005) .
- [11] T. H. Stievater, Xiaoqin Li, D. G. Steel, D. Gammon, D. S. Katzer, D. Park, C. Piermarocchi, and L. J. Sham, *Phys. Rev. Lett.* **87**, 133603 (2001).
- [12] L. Besombes, J. J. Baumberg, and J. Motohisa, *Phys. Rev. Lett.* **90**, 257402 (2003).
- [13] Yu. A. Pashkin, T. Yamamoto, O. Astafiev, Y. Nakamura, D. V. Averin, J. S. Tsai, *Nature* **421**, 823 (2003).
- [14] A. Zrenner, E. Beham, S. Stuffer, F. Findeis, M. Bichler, G. Abstreiter, *Nature* **418**, 612 (2002).
- [15] B. Krummheuer, V. M. Axt, and T. Kuhn, *Phys. Rev. B* **65**, 195313 (2002).
- [16] Milena Grifoni, Maura Sassetti, Jürgen Stockburger and Ulrich Weiss, *Phys. Rev. E* **48**, 3497 (1993).
- [17] H. Jirari and W. Pötz, *Phys. Rev. A* **74**, 022306 (2006).
- [18] Milena Grifoni, Maura Sassetti, Peter Hänggi and Ulrich Weiss, *Phys. Rev. E* **52**, 3596 (1995).
- [19] Ludwig Hartmann, Igor Goychuk, Milena Grifoni, and Peter Hänggi, *Phys. Rev. E* **61**, R4687 (2000).
- [20] Dmitrii E. Makarov and Nancy Makri, *Phys. Rev. E* **53**, 5863 (1995).
- [21] Feng Shuang, Chen Yang, Houyu Zhang, and YiJing Yan, *Phys. Rev. E* **61**, 7192 (2005).
- [22] P. Silvestrini and L. Stodolsky, *Phys. Lett. A* **280**, 17 (2001).
- [23] T. Brandes and T. Vorrath, *Phys. Rev. B* **66**, 075341 (2002).
- [24] Milena Grifoni and Peter Hänggi, *Phys. Rep.* **304**, 229 (1998).
- [25] Zheng, *Eur. Phys. J. B* **38**, 559 (2004).

- [26] Marlan O. Scully and M. Suhail Zubairy, *Quantum optics*, (World Scientific, Cambridge University, 2000).
- [27] Gerald D. Mahan, *Many-Partical physics*, (World Scientific, New York, 1990).
- [28] Milena Grifoni, Manfred Winterstetter, and Ulrich Weiss, Phys. Rev. E **56**, 334 (1997).
- [29] D. Vion, A. Aassime, A. Cottet, P. Joyez, H. Pothier, C. Urbina, D. Esteve, and M. H. Devoret, Science **296**, 886 (2002).
- [30] K. Shiokawa and B. L. Hu, Phys. Rev. A **70**, 062106 (2004).

FIGURES

Fig.1. The population difference $\langle\sigma_z(t)\rangle$ versus $\omega_c t$ in the initialization $\langle\sigma_z(t=0)\rangle = 1$ with various values of the driving field amplitude, $\varepsilon = 0, 0.01, 0.1, 0.4$, correspond to left panels (a) to (d). Also shown with the right panels are the Fourier spectrum with parameters same as the left panels. the coupling constant of the environment and TLS $\alpha = 0.01$ except (d) $\alpha = 0.3$. The driving field frequency near-resonance with TLS $\Omega = \Delta$.

Fig.2. The coherence $\langle\sigma_x(t)\rangle$ versus $\omega_c t$ in the initialization $\langle\sigma_z(t=0)\rangle = 1$ with various values of the driving field amplitude, $\varepsilon = 0$ (solid line), 0.01 (dashed line), 0.1 (dotted line), 0.4 (dot-dashed line).

Fig.3. The population difference versus $\omega_c t$ in the initialization $\langle\sigma_x(t=0)\rangle = 1$ with various values of the driving field amplitude, $\varepsilon = 0, 0.01, 0.1, 0.4$, correspond to left panels (a) to (d). Also shown with the right panels are the Fourier spectrum with parameters same as the left panels. the coupling constant of the environment and TLS $\alpha = 0.01$. The driving field frequency near-resonance with TLS $\Omega = \Delta$.

Fig.4 The coherence $\langle\sigma_x(t)\rangle$ versus $\omega_c t$ in the initialization $\langle\sigma_x(t=0)\rangle = 1$ with various values of the driving field amplitude. (a) $\varepsilon = 0$ (solid line), 0.01 (dashed line), 0.1 (dotted line), (b) 0.3, (c) 0.4.

Fig.5 $\text{ReD}(\omega)$ vs ω for different driving field amplitude $\varepsilon = 0$ (solid line), 0.1 (dashed line), 0.3 (dotted line), 0.5 (dot-dashed line).

Fig.1

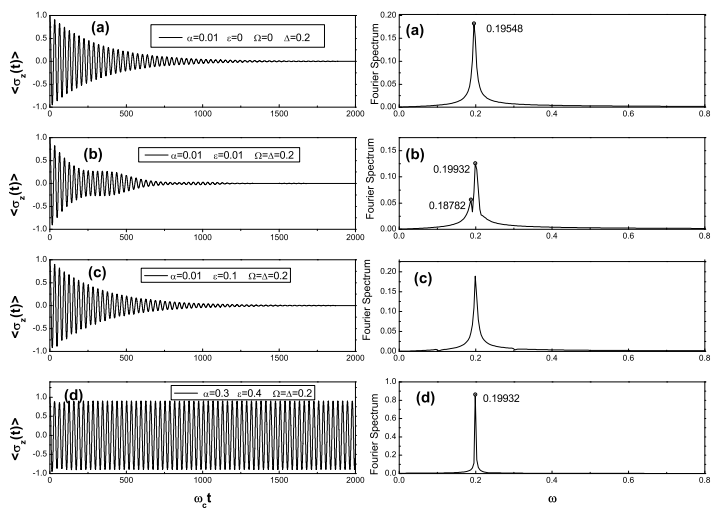


Fig.2

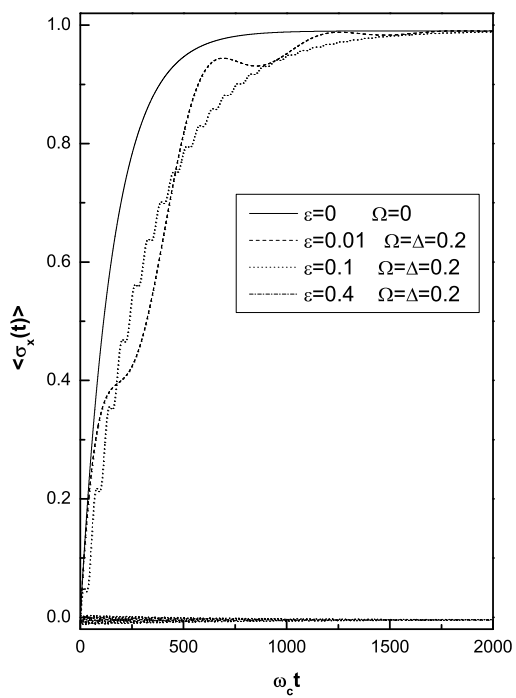


Fig.3

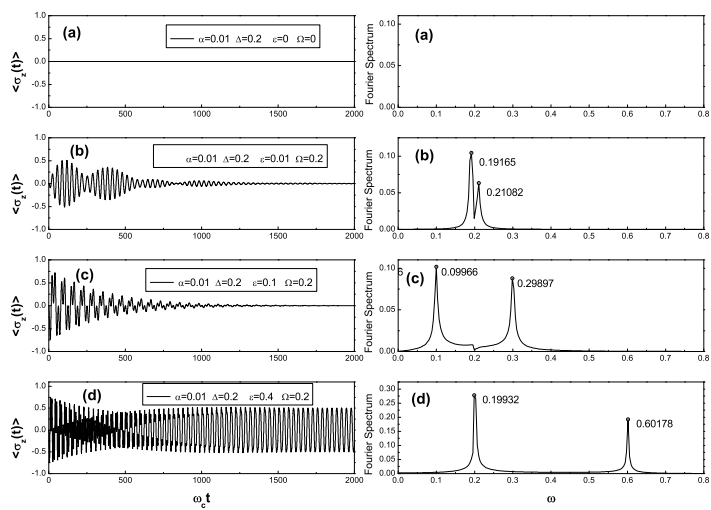


Fig.4

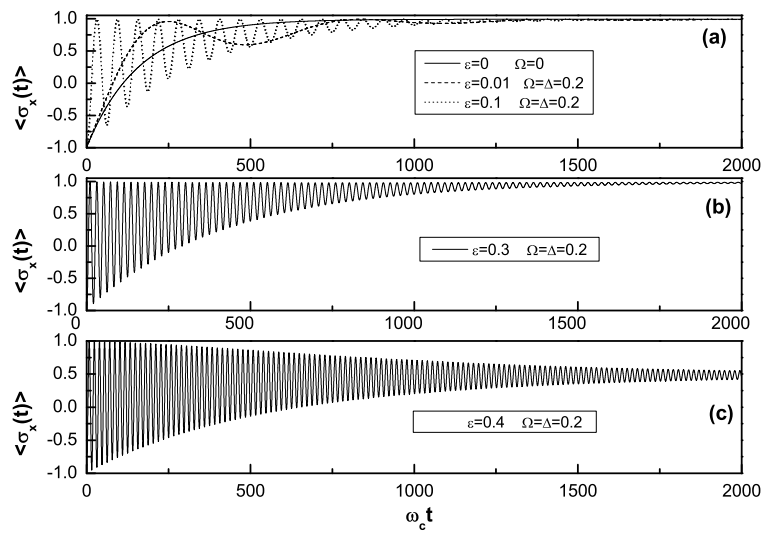


Fig.5

